OL | Organic Letters

Letter

Cite This: Org. Lett. XXXX, XXX, XXX−XXX

pubs.acs.org/OrgLett

Tetracoordinate Boron-Fused Double [5]Helicenes as Cathode Active Materials for Lithium Batteries

Susumu Oda, Takeshi Shimizu, Takazumi Katayama, Hirofumi Yoshikawa,* and Takuji Hatakeyama*

School of Science and Technology, Kwansei Gakuin University, 2-1 Gakuen, Sanda, Hyogo 669-1337, Japan

Supporting Information

ABSTRACT: Double [5]helicenes possessing two tetracoordinated boron atoms at the ring junctions were synthesized from glycine anhydride in three steps. The helicene with fluorine substituents on the boron atoms was employed as a cathode active material in a lithium battery to demonstrate moderate performance in the 1.8−3.5 V range with more than 63 mAh g^{-1} discharge capacity for 20 cycles and high Coulombic efficiency of over 90%.

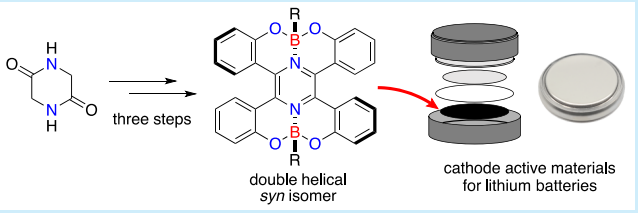

Tetracoordinate boron compounds have attracted significant attention because of their excellent photophysical properties,[1] which have led to numerous applications in optoelectronics, including organic light-emitting diodes (OLEDs),[2] organic field-effect transistors,[3] and photoresponsive materials.[4] To elicit diverse functionality, various types of chelate ligands for the boron center, such as N,N-, N,C-, and N,O-ligands, have been exploited. In particular, tetracoordinate boron compounds employing pyridyl phenolate as N,O-chelate ligands have proven to be promising light emission materials and electron transport materials for OLEDs.[5] In view of their potential utility, further exploration of such novel functions is highly desirable.

Helicenes are nonplanar screw-shaped molecules composed of *ortho*-fused aromatic rings.[6] Owing to their inherent chirality and dynamic behavior involving self-assembly, they offer many possible applications as asymmetric catalysts, molecular machines, and in molecular recognition and organic electronics. Recently, much effort has been devoted to accomplishing multihelicity, which leads to dramatic changes in physical properties as a result of increased distortion and multidimensional intermolecular interactions.[7,8] Despite the remarkable progress in the study of helicenes with multihelicity, multiple helicenes that possess tetracoordinated boron atoms have not been reported to date.[9] This is primarily because of a lack of suitable synthetic methods.

Herein, we report a three-step synthesis of tetracoordinate boron-fused double [5]helicenes, consisting of haloaromatization, Suzuki−Miyaura coupling, and demethylative borylation. The developed protocol is facile and scalable and provides access to derivatives with different substituents on the boron atoms by successive reaction with nucleophiles. Notably, a *syn*-racemic isomer was selectively obtained by preferential crystallization. Furthermore, the double helicene with fluorine substituents on the boron atoms showed reversible reduction, a property that can be exploited for preparing a cathode active material for lithium batteries with moderate capacity and cycle stability. To the best of our knowledge, this report presents the first example of a lithium battery employing tetracoordinate boron compounds as the electrode active material.[10,11]

The syntheses of **1a** and **1b** are summarized in Scheme 1. Glycine anhydride was exposed to phosphorus pentachloride and phosphoryl chloride to give tetrachloropyrazine in 63% yield. The palladium-catalyzed Suzuki−Miyaura coupling reaction of tetrachloropyrazine with 2-methoxyphenylboronic acid proceeded at 100 °C to afford tetraarylpyrazine **2** in 78% yield. In the presence of BBr_3, demethylation took place smoothly at 40 °C in toluene to form intermediate **3a**, which was then treated with phenylmagnesium bromide to give **1a** in 35% yield. Moreover, intermediate **3b** was formed by using BI_3, followed by addition of AgF, to afford **1b** in 45% yield. These compounds showed substantial chemical stability against acidic and basic conditions: no decomposition was observed on

Scheme 1. Synthesis of Tetracoordinate Boron-Fused Double Helicenes 1a and 1b

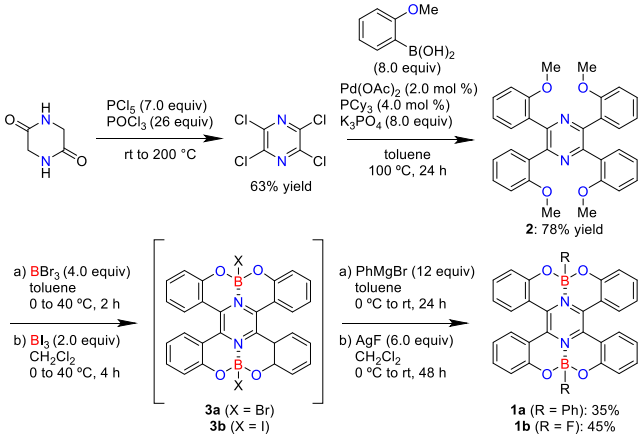

Received: January 26, 2019

DOI: 10.1021/acs.orglett.9b00337
Org. Lett. XXXX, XXX, XXX−XXX

treatment with 0.5 N HCl or NaOH aqueous solutions. However, gradual decomposition was observed during silica gel column chromatography, presumably as a result of the reaction between the B−O bonds and Si−OH groups on silica gel.

The ^{1}H NMR spectrum of **1a** shows eight peaks in the aromatic region, except for those of the phenyl substituents on the boron atoms. Given that four peaks should be observed from a single isomer, this result indicates that **1a** exists as a mixture of two isomers in 1:1 ratio (Figure 1). Based on the stereochemistry of the substituents on boron (*syn*/*anti*) and the helicenes (*P*/*M*), these double helicenes afforded four possible diastereomers (Figure 2): syn_racemic (*PP*/*MM*), syn_meso (*PM*), anti_racemic (*PP*/*MM*), and anti_meso (*PM*). Density functional theory calculations revealed that **syn_rac_1a** and **anti_rac_1a** were the most and second-most stable diastereomers, respectively. The *meso* diastereomers were relatively unstable (6.27 and 2.77 kcal/mol, respectively), which is commonly observed in highly fused double helicenes.[9c−e] Owing to the small energy difference (0.05 kcal/mol) between **syn_rac_1a** and **anti_rac_1a**, they were identified as the two observed isomers.

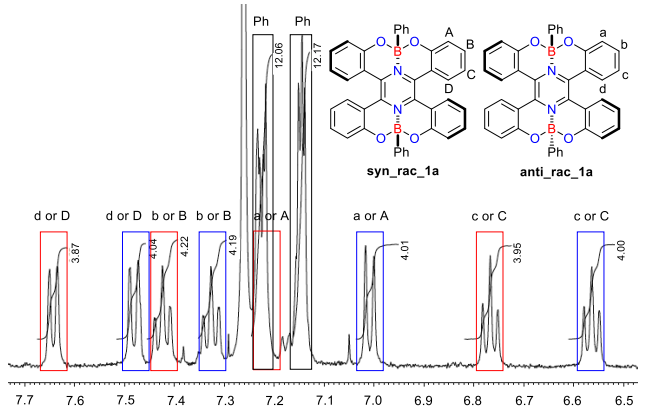

Figure 1. ^{1}H NMR spectrum of **1a** in $CDCl_3$ at 25 °C.

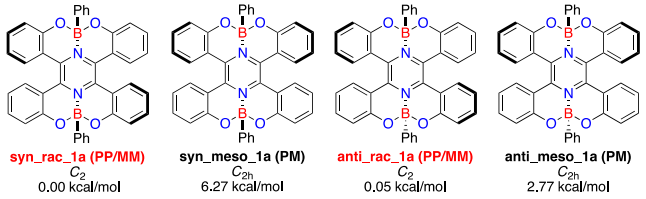

Figure 2. Relative electron energies (Δ*E*) of **1a** diastereomers calculated at the B3LYP/6-31G(d) level of theory.

The helical structure of **syn_rac_1a** was determined by X-ray crystallography (Figure 3). The four coordinated boron atoms of **syn_rac_1a** adopt a tetrahedral geometry. The B−C, B−O, and B−N bond lengths are 1.618, 1.451−1.467, and 1.605−1.611 Å, respectively, which are comparable to those of reported phenol−pyridyl boron complexes.[5c] Although the C3−C3′ and C3−N1 bond lengths are similar to those of the reported pyrazine ring, the dihedral angles between the planes of the terminal rings (A−A′, 40.4°; B−B′, 51.9°) indicate low aromaticity of the central pyrazine ring because of strong distortion. This observation is consistent with the relatively small nucleus-independent chemical shift (NICS(0)) value of −1.9 (Figure S6).

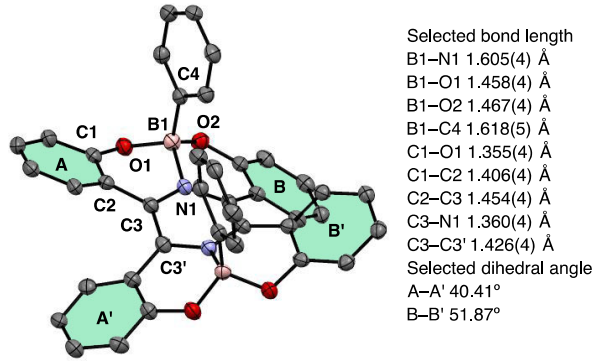

Figure 3. ORTEP drawing of **syn_rac_1a** obtained by X-ray crystallographic analysis. Thermal ellipsoids are shown at 50% probability. Hydrogen atoms are omitted for clarity.

Notably, recrystallization of **1a** from benzene gave only a single crystal of **syn_rac_1a**. Although ^{1}H NMR analysis indicated the existence of **anti_rac_1a**, its single crystal was not obtained despite multiple attempts using various solvents (benzene, dichloromethane, toluene, diethyl ether, dioxane, and carbon tetrachloride). This suggests that **1a** preferentially crystallizes as **syn_rac_1a** under rapid equilibrium between *syn*- and *anti*-racemic isomers in the solution state. The single crystal of **syn_rac_1a** was then subjected to ^{1}H NMR spectroscopy in $CDCl_3$ at low temperature (−40 °C), which revealed a mixture of the two isomers in a 1:1 ratio. To confirm the stereochemistry of **1a** in the solid state, powder X-ray diffraction (XRD) analysis of the solid obtained after simple evaporation was performed (Figure S2). The powder XRD pattern of **1a** is in good agreement with that simulated from the single-crystal data of **syn_rac_1a**. Based on these results, we conclude that **1a** is in rapid equilibrium between the *syn*- and *anti*-racemic isomers in the solution state but forms the *syn*-racemic isomer in the solid state. We assume that the rapid isomerization proceeds through the cleavage of the B−N or B−O bond. Similar results were obtained with **1b** by means of ^{1}H NMR analysis, DFT calculations, and X-ray crystallographic analysis (Figures S1, S4, and S18).

The photophysical properties of **1a** and **1b** in CH_2Cl_2 are summarized in Figure 4. The absorption maxima of **1a** and **1b** were 574 and 553 nm, respectively. Time-dependent DFT calculations suggest that the absorption bands of **1a** and **1b** correspond to the S_0−S_1 transitions of the *syn*-racemic (*PP*/*MM*) and *anti*-racemic (*PP*/*MM*) isomers because their excitation energies are almost identical (**syn_rac_1a**, 2.14 eV; **anti_rac_1a**, 2.17 eV; **syn_rac_1b**, 2.26 eV; **anti_rac_1b**, 2.29 eV; Tables S1 and S2). They showed red emission bands at 653 and 623 nm (Φ_f = 0.20, 0.29), respectively.

The electrochemical properties of **1a** and **1b** were studied by cyclic voltammetry (Figure S5). One reversible reduction wave was observed for **1a** ($E_{1/2}^{red}$ = −1.06 V), whereas two reversible reduction waves were observed for **1b** ($E_{1/2}^{red}$ = −0.97 and −1.64 V). The second reduction wave of **1a** was not observed within a potential window of CH_2Cl_2 (ca. −2.0 V). The two-electron reduction of **1b** is not attributed to the two diastereomers because the LUMO energy levels of **syn_rac_1b** (−3.00 eV) and **anti_rac_1b** (−2.93 eV) are very close and cannot be distinguished by cyclic voltammetry. Encouraged by the reduction property and low LUMO energy level of **1b**, we

DOI: 10.1021/acs.orglett.9b00337
Org. Lett. XXXX, XXX, XXX−XXX

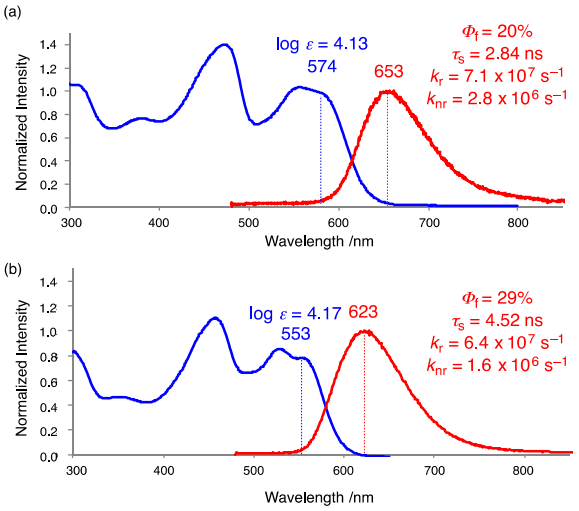

Figure 4. Normalized absorption (red) and fluorescence (blue) spectra of (a) **1a** and (b) **1b** (0.02 mM in CH_2Cl_2) with photophysical data. Abbreviations: ε, absorption coefficient at absorption maximum; Φ_f, absolute PL quantum yield; τ_s, fluorescence lifetime measured at an emission maximum; k_r, radiative rate constant; k_{nr}, nonradiative rate constant.

investigated its performance as an electrode active material for lithium batteries.

After careful screening of the electrolytes, lithium bis(trifluoromethanesulfonyl)imide (LiTFSI) in ionic liquid, 1,2-dimethyl-3-propylimidazolium bis(trifluoromethanesulfonyl)imide (DMPImTFSI),[12] was found to afford a stable cycle performance owing to its low solubility, which suppressed the dissolution of the cathode active material into the electrolyte solution (Figure 5). The discharge curve showed a long plateau at 2.2 V in the first cycle but exhibited a gentle slope between 3.0 and 3.2 V after the second cycle. This result correlates well with the reduction potentials of the corresponding battery of **1b**, as determined by cyclic voltammetry ($E_{1/2}^{red}$ = 2.1, 3.1 V) (Figure S9). The initial discharge capacity (180 mAh g^{-1}) was much higher than the theoretical capacity (106 mAh g^{-1}), although the subsequent discharge capacities were close to the theoretical capacity, and a long plateau was not observed after the second discharge process. Moreover, the Coulombic efficiency at the first cycle exceeded 180%, which indicates that the initial process is irreversible due to electrolyte decomposition and solid-electrolyte interface formation and is peculiar to ionic liquids.[13] Therefore, to evaluate the battery performance of **1b**, the discharge curves were obtained after the second discharge process. The second discharge capacity of **1b** was 93 mAh g^{-1}, which corresponds to 88% of the theoretical capacity, and the capacity retention after the 20th discharge process was 67%. Moreover, high Coulombic efficiency of more than 90% was maintained between the second and 20th processes. Notably, tetraarylpyrazine **2** did not show the redox property and the battery performance (Figures S11 and S12).

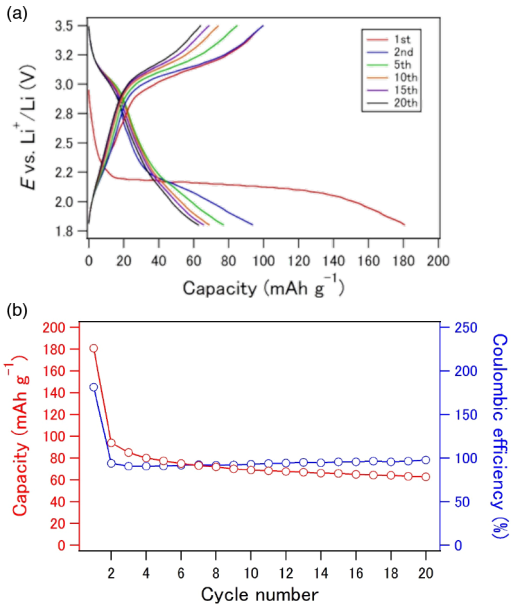

Figure 5. (a) Discharge−charge curves of **1b** during 20 cycles. (b) Cycle performance of **1b**. LiTFSI/DMPImTFSI was used as an electrolyte.

In summary, we synthesized tetracoordinate boron-fused double [5]helicenes through demethylative borylation and successive treatment with nucleophiles such as Grignard reagents and silver fluoride. Stereoselective formation of *syn*-racemic isomer through preferential crystallization was confirmed by X-ray crystallography. These double helicenes showed strong red emissions and reversible reduction waves. In particular, the double helicene with fluorine substituents exhibited two reversible reductions and a low LUMO energy level. The lithium battery fabricated using this helicene as the cathode active material showed moderate performance, capacity, and cycle stability. The key to success is the use of an ionic liquid as the electrolyte to suppress the leaching of the electrode active material. These results not only extend the feasibility of organic electrode materials for lithium batteries but also encourage the further development of organoboron-based materials.

■ ASSOCIATED CONTENT

Supporting Information

The Supporting Information is available free of charge on the ACS Publications website at DOI: 10.1021/acs.orglett.9b00337.

Synthesis, analytical data, NMR spectra, DFT studies, CV measurements, X-ray crystallography, fabrication of lithium battery (PDF)

Accession Codes

CCDC 1890482 and 1890488 contain the supplementary crystallographic data for this paper. These data can be obtained free of charge via www.ccdc.cam.ac.uk/data_request/cif, or by emailing data_request@ccdc.cam.ac.uk, or by contacting The Cambridge Crystallographic Data Centre, 12 Union Road, Cambridge CB2 1EZ, UK; fax: +44 1223 336033.

■ AUTHOR INFORMATION

Corresponding Authors

*E-mail: yoshikawah@kwansei.ac.jp.
*E-mail: hatake@kwansei.ac.jp.

ORCID

Susumu Oda: 0000-0003-1088-1932
Takuji Hatakeyama: 0000-0002-7483-9525

Notes

The authors declare no competing financial interest.

DOI: 10.1021/acs.orglett.9b00337
Org. Lett. XXXX, XXX, XXX−XXX

■ ACKNOWLEDGMENTS

This study was supported by a Grant-in-Aid for Scientific Research on Innovative Areas "π-System Figuration" (JP17H05164), Grant-in-Aid for Scientific Research (JP18H02051), Challenging Research (Exploratory, JP17K19164), and Grant-in-Aid for Early-Career Scientists (18K14228) from the Japan Society for the Promotion of Science (JSPS), Iketani Science and Technology Foundation, Mitsubishi Foundation, Sumitomo Foundation, and Foundation of Kinoshita Memorial Enterprise. Preliminary measurements of the X-ray crystal structure analysis were performed at BL40XU in the SPring-8 with the approval of JASRI (2016A1052, 2016B1059, 2017A1132, 2017B1073, 2018A1114) and with the help of Dr. Nobuhiro Yasuda (JASRI) and Mr. Soichiro Nakatsuka (Kwansei Gakuin University). Powder X-ray diffraction analysis was performed with the help of Prof. Daisuke Tanaka and Mr. Yoshinobu Kamakura (Kwansei Gakuin University). We are grateful to Mr. Yasuhiro Kondo (JNC Petrochemical Corp.) for providing experimental support.

■ REFERENCES

(1) (a) Rao, Y.-L.; Wang, S. *Inorg. Chem.* **2011**, *50*, 12263. (b) Li, D.; Zhang, H.; Wang, Y. *Chem. Soc. Rev.* **2013**, *42*, 8416. (c) Frath, D.; Massue, J.; Ulrich, G.; Ziessel, R. *Angew. Chem., Int. Ed.* **2014**, *53*, 2290.

(2) (a) Chang, Y.-L.; Rao, Y.-L.; Gong, S.; Ingram, G. L.; Wang, S.; Lu, Z.-H. *Adv. Mater.* **2014**, *26*, 6729. (b) Shiu, Y.-J.; Cheng, Y.-C.; Tsai, W.-L.; Wu, C.-C.; Chao, C.-T.; Lu, C.-W.; Chi, Y.; Chen, Y.-T.; Liu, S.-H.; Chou, P.-T. *Angew. Chem., Int. Ed.* **2016**, *55*, 3017. (c) Matsuo, K.; Yasuda, T. *Chem. Commun.* **2017**, *53*, 8723. (d) Fukagawa, H.; Sasaki, T.; Tsuzuki, T.; Nakajima, Y.; Takei, T.; Motomura, G.; Hasegawa, M.; Morii, K.; Shimizu, T. *Adv. Mater.* **2018**, *30*, 1706768. (e) Mamada, M.; Tian, G.; Nakanotani, H.; Su, J.; Adachi, C. *Angew. Chem., Int. Ed.* **2018**, *57*, 12380.

(3) (a) Sun, Y.; Rohde, D.; Liu, Y.; Wan, L.; Wang, Y.; Wu, W.; Di, C.; Yu, G.; Zhu, D. *J. Mater. Chem.* **2006**, *16*, 4499. (b) Yasuda, T.; Tsutsui, T. *Mol. Cryst. Liq. Cryst.* **2006**, *462*, 3. (c) Ono, K.; Yamaguchi, H.; Taga, K.; Saito, K.; Nishida, J.; Yamashita, Y. *Org. Lett.* **2009**, *11*, 149. (d) Sheng, W.; Zheng, Y.-Q.; Wu, Q.; Wu, Y.; Yu, C.; Jiao, L.; Hao, E.; Wang, J.-Y.; Pei, J. *Org. Lett.* **2017**, *19*, 2893. (e) Hecht, R.; Kade, J.; Schmidt, D.; Nowak-Król, A. *Chem. - Eur. J.* **2017**, *23*, 11620.

(4) (a) Baik, C.; Murphy, S. K.; Wang, S. *Angew. Chem., Int. Ed.* **2010**, *49*, 8224. (b) Nagura, K.; Saito, S.; Fröhlich, R.; Glorius, F.; Yamaguchi, S. *Angew. Chem., Int. Ed.* **2012**, *51*, 7762. (c) Rao, Y.-L.; Chen, L. D.; Mosey, N. J.; Wang, S. *J. Am. Chem. Soc.* **2012**, *134*, 11026. (d) Rao, Y.-L.; Amarne, H.; Chen, L. D.; Brown, M. L.; Mosey, N. J.; Wang, S. *J. Am. Chem. Soc.* **2013**, *135*, 3407. (e) Iida, A.; Saito, S.; Sasamori, T.; Yamaguchi, S. *Angew. Chem., Int. Ed.* **2013**, *52*, 3760.

(5) (a) Li, Y.; Liu, Y.; Bu, W.; Guo, J.; Wang, Y. *Chem. Commun.* **2000**, 1551. (b) Liu, Y.; Guo, J.; Zhang, H.; Wang, Y. *Angew. Chem., Int. Ed.* **2002**, *41*, 182. (c) Zhang, H.; Huo, C.; Ye, K.; Zhang, P.; Tian, W.; Wang, Y. *Inorg. Chem.* **2006**, *45*, 2788. (d) Zhang, H.; Huo, C.; Zhang, J.; Zhang, P.; Tian, W.; Wang, Y. *Chem. Commun.* **2006**, 281. (e) Zhang, Z.; Yao, D.; Zhao, S.; Gao, H.; Fan, Y.; Su, Z.; Zhang, H.; Wang, Y. *Dalton Trans* **2010**, *39*, 5123.

(6) (a) Shen, Y.; Chen, C.-F. *Chem. Rev.* **2012**, *112*, 1463. (b) Gingras, M. *Chem. Soc. Rev.* **2013**, *42*, 968. (c) Gingras, M.; Félix, G.; Peresutti, R. *Chem. Soc. Rev.* **2013**, *42*, 1007. (d) Gingras, M. *Chem. Soc. Rev.* **2013**, *42*, 1051. (e) Peng, Z.; Takenaka, N. *Chem. Rec.* **2013**, *13*, 28. (f) Yamaguchi, M.; Shigeno, M.; Saito, N.; Yamamoto, K. *Chem. Rec.* **2014**, *14*, 15. (g) Tanaka, K.; Kimura, Y.; Murayama, K. *Bull. Chem. Soc. Jpn.* **2015**, *88*, 375. (h) Li, C.; Yang, Y.; Miao, Q. *Chem. - Asian J.* **2018**, *13*, 884.

(7) (a) Pena, D.; Cobas, A.; Perez, D.; Guitian, E.; Castedo, L. *Org. Lett.* **2003**, *5*, 1863. (b) Chen, T.-A.; Liu, R.-S. *Org. Lett.* **2011**, *13*, 4644. (c) Lütke Eversloh, C.; Liu, Z.; Müller, B.; Stangl, M.; Li, C.; Müllen, K. *Org. Lett.* **2011**, *13*, 5528. (d) Luo, J.; Xu, X.; Mao, R.; Miao, Q. *J. Am. Chem. Soc.* **2012**, *134*, 13796. (e) Xiao, S.; Kang, S. J.; Wu, Y.; Ahn, S.; Kim, J. B.; Loo, Y.-L.; Siegrist, T.; Steigerwald, M. L.; Li, H.; Nuckolls, C. *Chem. Sci.* **2013**, *4*, 2018. (f) Zhong, Y.; Kumar, B.; Oh, S.; Trinh, M. T.; Wu, Y.; Elbert, K.; Li, P.; Zhu, X.; Xiao, S.; Ng, F.; Steigerwald, M. L.; Nuckolls, C. *J. Am. Chem. Soc.* **2014**, *136*, 8122. (g) Kashihara, H.; Asada, T.; Kamikawa, K. *Chem. - Eur. J.* **2015**, *21*, 6523. (h) Ball, M.; Zhong, Y.; Wu, Y.; Schenck, C.; Ng, F.; Steigerwald, M.; Xiao, S.; Nuckolls, C. *Acc. Chem. Res.* **2015**, *48*, 267. (i) Fujikawa, T.; Segawa, Y.; Itami, K. *J. Am. Chem. Soc.* **2015**, *137*, 7763. (j) Berezhnaia, V.; Roy, M.; Vanthuyne, N.; Villa, M.; Naubron, J.-V.; Rodriguez, J.; Coquerel, Y.; Gingras, M. *J. Am. Chem. Soc.* **2017**, *139*, 18508. (k) Hosokawa, T.; Takahashi, Y.; Matsushima, T.; Watanabe, S.; Kikkawa, S.; Azumaya, I.; Tsurusaki, A.; Kamikawa, K. *J. Am. Chem. Soc.* **2017**, *139*, 18512. (l) Berezhnaia, V.; Roy, M.; Vanthuyne, N.; Villa, M.; Naubron, J.-V.; Rodriguez, J.; Coquerel, Y.; Gingras, M. *J. Am. Chem. Soc.* **2017**, *139*, 18508. (m) Kato, K.; Segawa, Y.; Scott, L. T.; Itami, K. *Angew. Chem., Int. Ed.* **2018**, *57*, 1337. (n) Zhu, Y.; Xia, Z.; Cai, Z.; Yuan, Z.; Jiang, N.; Li, T.; Wang, Y.; Guo, X.; Li, Z.; Ma, S.; Zhong, D.; Li, Y.; Wang, J. *J. Am. Chem. Soc.* **2018**, *140*, 4222.

(8) (a) Shiraishi, K.; Rajca, A.; Pink, M.; Rajca, S. *J. Am. Chem. Soc.* **2005**, *127*, 9312. (b) Wang, Z.; Shi, J.; Wang, J.; Li, C.; Tian, X.; Cheng, Y.; Wang, H. *Org. Lett.* **2010**, *12*, 456. (c) Liu, X.; Yu, P.; Xu, L.; Yang, J.; Shi, J.; Wang, Z.; Cheng, Y.; Wang, H. *J. Org. Chem.* **2013**, *78*, 6316. (d) Hashimoto, S.; Nakatsuka, S.; Nakamura, M.; Hatakeyama, T. *Angew. Chem., Int. Ed.* **2014**, *53*, 14074. (e) Nakamura, K.; Furumi, S.; Takeuchi, M.; Shibuya, T.; Tanaka, K. *J. Am. Chem. Soc.* **2014**, *136*, 5555. (f) Sakamaki, D.; Kumano, D.; Yashima, E.; Seki, S. *Angew. Chem., Int. Ed.* **2015**, *54*, 5404. (g) Sakamaki, D.; Kumano, D.; Yashima, E.; Seki, S. *Chem. Commun.* **2015**, *51*, 17237. (h) Fujikawa, T.; Segawa, Y.; Itami, K. *J. Am. Chem. Soc.* **2016**, *138*, 3587. (i) Gulevskaya, A. V.; Shvydkova, E. A.; Tonkoglazova, D. I. *Eur. J. Org. Chem.* **2018**, *2018*, 5030.

(9) Helicenes and multiple helicenes with tricoordinate boron atoms: (a) Hatakeyama, T.; Hashimoto, S.; Oba, T.; Nakamura, M. *J. Am. Chem. Soc.* **2012**, *134*, 19600. (b) Hirai, H.; Nakajima, K.; Nakatsuka, S.; Shiren, K.; Ni, J.; Nomura, S.; Ikuta, T.; Hatakeyama, T. *Angew. Chem., Int. Ed.* **2015**, *54*, 13581. (c) Katayama, T.; Nakatsuka, S.; Hirai, H.; Yasuda, N.; Kumar, J.; Kawai, T.; Hatakeyama, T. *J. Am. Chem. Soc.* **2016**, *138*, 5210. (d) Wang, X.-Y.; Narita, A.; Zhang, W.; Feng, X.; Müllen, K. *J. Am. Chem. Soc.* **2016**, *138*, 9021. (e) Wang, X.-Y.; Wang, X.-C.; Narita, A.; Wagner, M.; Cao, X.-Y.; Feng, X.; Müllen, K. *J. Am. Chem. Soc.* **2016**, *138*, 12783. (f) Matsui, K.; Oda, S.; Yoshiura, K.; Nakajima, K.; Yasuda, N.; Hatakeyama, T. *J. Am. Chem. Soc.* **2018**, *140*, 1195.

(10) Tricoordinate boron-based electrode active material: (a) Wu, Z.-S.; Ren, W.; Xu, L.; Li, F.; Cheng, H.-M. *ACS Nano* **2011**, *5*, 5463. (b) Osumi, S.; Saito, S.; Dou, C.; Matsuo, K.; Kume, K.; Yoshikawa, H.; Awaga, K.; Yamaguchi, S. *Chem. Sci.* **2016**, *7*, 219.

(11) (a) Liang, L.; Tao, Z.; Chen, J. *Adv. Energy Mater.* **2012**, *2*, 742. (b) Xie, J.; Zhang, Q. *J. Mater. Chem. A* **2016**, *4*, 7091. (c) Schon, T. B.; McAllister, B. T.; Li, P.-F.; Seferos, D. S. *Chem. Soc. Rev.* **2016**, *45*, 6345. (d) Kim, K. C. *Ind. Eng. Chem. Res.* **2017**, *56*, 12009.

(12) Seki, S.; Kobayashi, Y.; Miyashiro, H.; Ohno, Y.; Usami, A.; Mita, Y.; Kihira, N.; Watanabe, M.; Terada, N. *J. Phys. Chem. B* **2006**, *110*, 10228.

(13) (a) Zhao, X.; Zhao-Karger, Z.; Wang, D.; Fichtner, M. *Angew. Chem., Int. Ed.* **2013**, *52*, 13621. (b) Gurkan, B. E.; Qiang, Z.; Chen, Y.-M.; Zhu, Y.; Vogt, B. D. *J. Electrochem. Soc.* **2017**, *164*, H5093.

DOI: 10.1021/acs.orglett.9b00337
Org. Lett. XXXX, XXX, XXX−XXX